

## Article

# Effect of Heat Treatment on Some Titanium Alloys Used as Biomaterials

Madalina Simona Baltatu <sup>1</sup>, Cristiana Chiriac-Moruzzi <sup>1</sup>, Petrica Vizureanu <sup>1,2,\*</sup>, László Tóth <sup>3</sup> and János Novák <sup>4</sup>

<sup>1</sup> Department of Technologies and Equipments for Materials Processing, Faculty of Materials Science and Engineering, Gheorghe Asachi Technical University of Iași, Blvd. Mangeron, No. 51, 700050 Iași, Romania

<sup>2</sup> Technical Sciences Academy of Romania, Dacia Blvd 26, 030167 Bucharest, Romania

<sup>3</sup> Bánki Donát Faculty of Mechanical and Safety Engineering, Óbuda University, Bécsi út 96/B, 1034 Budapest, Hungary

<sup>4</sup> Doctoral School on Safety and Security Sciences, Óbuda University, Bécsi út 96/B, 1034 Budapest, Hungary

\* Correspondence: peviz@tuiasi.ro

**Abstract:** Titanium-based alloys are constantly improved to obtain properties suitable for their use. Improving titanium alloys is very important for performing alloys without side effects. In this paper effects of structure, microhardness, and indentation test of eight titanium alloys were investigated after aging. The heat treatment consisted of a high-temperature quenching accomplished in three steps (650 °C for 25 min, 850 °C for 20 min, and 950 °C for 20 min). The cooling process was accomplished using N<sub>2</sub> gas, introduced in the chamber at a 9-bar pressure for 37 min. Then, followed by heating to a constant temperature tempering (550 °C) at 1.5 bar pressure and kept for 2 h and 10 min at 2 bar pressure. Optical microscopy images were obtained of Ti-Mo-Zr-Ta alloys with grain-specific aspects of titanium alloys; acicular and coarse structures are specific to  $\beta$  alloys. Microhardness results showed significantly influenced by the heat treatment, increased by approximately 5% for Ti15Mo7Zr15Ta1Si and Ti20Mo7Zr15Ta0.5Si, while for Ti15Mo7Zr15Ta0.5Si and Ti20Mo7Zr15Ta an approximately 9% decrease has been noted. The modulus of elasticity results obtained by the indentation method for the experimental alloys were between 36.25–66.24 GPa. The heat treatments applied to the alloys had a pronounced effect, improving both the structure of the alloys and the results of the indentation test.

**Keywords:** biomaterials; titanium-alloys; heat-treatment; microscopy; microhardness



**Citation:** Baltatu, M.S.; Chiriac-Moruzzi, C.; Vizureanu, P.; Tóth, L.; Novák, J. Effect of Heat Treatment on Some Titanium Alloys Used as Biomaterials. *Appl. Sci.* **2022**, *12*, 11241. <https://doi.org/10.3390/app122111241>

Academic Editor: Chiara Soffritti

Received: 12 October 2022

Accepted: 4 November 2022

Published: 6 November 2022

**Publisher's Note:** MDPI stays neutral with regard to jurisdictional claims in published maps and institutional affiliations.



**Copyright:** © 2022 by the authors. Licensee MDPI, Basel, Switzerland. This article is an open access article distributed under the terms and conditions of the Creative Commons Attribution (CC BY) license (<https://creativecommons.org/licenses/by/4.0/>).

## 1. Introduction

Biomaterials play an essential role in medicine today by restoring function and facilitating the healing of people after various accidents or diseases. These materials used for medical applications ensure appropriate treatment from a medical point of view and improve the quality of life through performance devices [1].

Due to their excellent properties, titanium and its alloys are still the most used materials in medical applications. They are mainly used in hard tissue replacement, and the fields of use are orthopedics, dentistry, and cardiovascular medicine [2–4].

In recent years, the utilization of titanium and titanium-based alloys with applications in biology and medicine has made tremendous progress promoting of innovative technologies and new materials [5]. Titanium-based alloys are distributed in three categories:  $\alpha$ ,  $\alpha + \beta$  and  $\beta$  alloys [6]. Reduced modulus of elasticity, greater corrosion resistance, and improved biocompatibility are all advantages of adding benign elements like Mo, Si, Zr, and Ta [7]. This is due to their superior mechanical, physical, and biological properties. New titanium alloys with harmless elements, long-term performance, and no rejection by the human body are being promoted in the present era. Other benefits include high specific strength, low density, and almost non-magnetic properties [8].

Titanium makes up roughly 0.5 percent of the Earth's crust. Titanium is a lightweight, high-strength, low-corrosion structural metal utilized in biocompatible materials as an alloy [9]. Pure titanium is ductile, electrically and thermally inert, and paramagnetic. Due to the production of a passive oxide surface coating, titanium has good corrosion resistance in a variety of conditions. It is biocompatible because of its great strength, low density, and exceptional corrosion resistance [10].

Titanium castings exhibit common casting defects like shrinkage, gas porosity, cold shuts and misruns. The surface defects, such as surface-connected porosity or cold shuts, can be improved with heat treatments [11].

Thermal and thermochemical treatments play an important role in achieving quality characteristics to obtain a certain complex of technological and/or use properties. Over time, various improvements of biocompatible materials have been opted for in order to obtain suitable properties for the human body [12–14].

Numerous types of research have confirmed that thermal treatments are beneficial for improving the properties of titanium alloys, Mo element significantly affects the  $\alpha$  microtexture of  $\alpha + \beta$  titanium alloys; strong prior  $\alpha$  colony microtexture exists before thermal deformation; the smaller  $\alpha$  colony will hinder the formation of a large-size microtexture [15,16].

The term “biocompatibility” refers to the interaction of a medical device's tissues and physiological systems with the tissues and physiological systems of the patient. Any device's overall safety evaluation includes a biocompatibility examination [17–19]. When choosing alloys for medical implants, in addition to the mechanical properties, biocompatibility is also an important aspect to consider, specifically the biocompatibility of the elements that make up the alloy. The alloys from the Ti-Mo-Zr-Ta system contain biocompatible elements, the cytotoxicity of the elements being demonstrated by other researchers [2,5,13]; the overall benefits of each element are highlighted in Table 1, both in the human body and in the sampled alloys [20].

**Table 1.** Benefits of the elements in the human body from Ti-Mo-Zr-Ta-Si system.

Element	Benefits	Toxicity Level
Ti— Titanium	- is not rejected by the human body - maintains good physical connections with the bone	Non-toxic
Mo— Molybdenum	- is important for enzymes in the cellular metabolism - low concentrations in the vertebrae	Low toxicity (compared to Co, Cr and Ni)
Zr— Zirconium	- no biological role - strong resistance to corrosion - highest biocompatibility of all metals	Low toxicity
Ta— Tantalum	- no biological role - strong resistance to corrosion - used for most biocompatible implants	Non-toxic
Si— Silicon	- found in natural bone - is important for growth and bone calcification	Low toxicity

In the literature research, many articles were found on titanium alloys being used in orthopedic and aerospace applications, being studied the microstructure, hardness, and biocompatibility properties in the cast form of the alloys [2,3]. However, a proper study investigating the heat treatment process, microstructure, and mechanical properties relationship for this Ti-Mo-Zr-Ta system has not been found [15,16]. For this reason, tests were performed on the thermally treated Ti-Mo-Zr-Ta system, and the microstructure and some mechanical properties that were modified due to the thermal treatment were examined.

Eight alloys based on Ti-Mo-Zr-Ta, six with Si, were thermally treated and investigated to improve the properties of titanium alloys. This study highlights the microstructural and

mechanical characteristics of experimental titanium alloys that have been heat-treated. After the heat treatment, the samples were analyzed using optical microscopy, microhardness testing, and an indentation test.

## 2. Materials and Methods

### 2.1. Material Preparation

Materials analyzed are from the Ti-Mo-Zr-Ta system, eight alloys developed in a Vacuum Arc Remelting installation [20–22]; six contain Si. In this paper, for obtaining the biocompatible Ti-Mo-Ta-Zr-Si alloys, high-purity chemical elements were used, raw materials such as Ti (99%), Mo (99%), Zr (99%), Ta (99%), and Si (99%) from Sigma-Aldrich. Table 2 shows the experimental alloys investigated in this paper.

**Table 2.** Chemical composition for Ti-Mo-Zr-Ta alloys obtained.

Alloy	Average Chemical Composition (wt.%)				
	Ti	Mo	Zr	Ta	Si
Ti15Mo7Zr15Ta	73.85 ± 0.3	9.00 ± 0.1	7.15 ± 0.2	10.00 ± 0.2	-
Ti15Mo7Zr15Ta0.5Si	66.50 ± 0.1	11.00 ± 0.2	7.00 ± 0.3	15.00 ± 0.1	0.50 ± 0.3
Ti15Mo7Zr15Ta0.75Si	66.20 ± 0.1	9.00 ± 0.3	7.00 ± 0.1	17.00 ± 0.3	0.80 ± 0.3
Ti15Mo7Zr15Ta1Si	73.00 ± 0.1	10.00 ± 0.2	8.00 ± 0.1	8.00 ± 0.2	1.00 ± 0.3
Ti20Mo7Zr15Ta	58.35 ± 0.1	19.00 ± 0.2	8.15 ± 0.1	14.50 ± 0.3	-
Ti20Mo7Zr15Ta0.5Si	59.25 ± 0.2	18.50 ± 0.3	7.00 ± 0.1	14.80 ± 0.1	0.45 ± 0.1
Ti20Mo7Zr15Ta0.75Si	57.86 ± 0.1	19.50 ± 0.1	6.85 ± 0.1	15.04 ± 0.3	0.75 ± 0.1
Ti20Mo7Zr15Ta1Si	57.23 ± 0.1	19.83 ± 0.3	6.93 ± 0.1	14.98 ± 0.2	1.03 ± 0.1

### 2.2. Heat Treatment

Some characteristics can be achieved with the help of thermal treatments known under the generic name of annealing. They are applied to semi-finished products obtained by casting, hot or cold plastic deformation (free forging or in a mold, lamination, extruding, drawing), or welded (metal constructions, machine parts, complex tools). The heat treatment for the Ti-Mo-Zr-Ta alloys has been realized using the IU 72/1F 2RV 60 × 60 × 40 10 bar CP type I vacuum furnace (IVA Schmetz GmbH, Menden, Germany) [23]. The hot zone, heat exchanger, high-capacity radial fan with an electric motor, and gas conduits are all included within the casing. The furnace's loading and unloading are done from the front using a rail-guided loading car to precisely place the cargo into the hot zone, as presented in Figure 1.

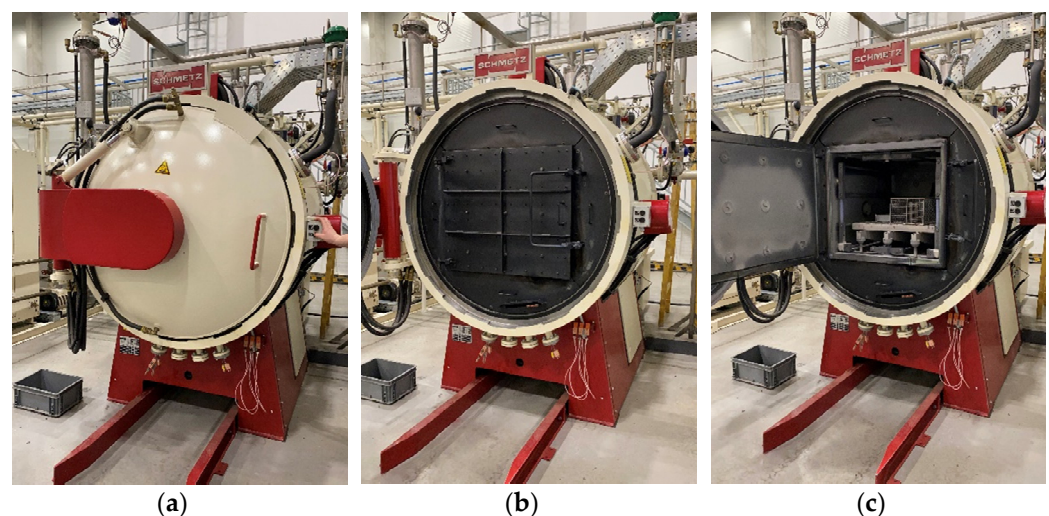


**Figure 1.** Horizontal high-temperature vacuum chamber furnace: (a) furnace front-view, (b) furnace set-up, (c) furnace chamber and sample holder.

After loading, the swiveling furnace door will be hydraulically fastened to the furnace casing to prevent overpressure. After that, the treatment cycle runs completely on its own [14]. The furnace has an operating system that allows the user to program each treatment step, considering factors such as temperature, cooling rate, gas pressure, ventilation etc.

### 2.3. Microstructural Characterization Methods

Optical Microscopy analyses on Ti-Mo-Zr-Ta alloys were performed with a DSX1000 Digital Microscope (Olympus Corporation, Tokyo, Japan). For microscopic examination, obtaining a suitable sample surface involves a series of operations: embedding with CITOPRESS-1 (Struers ApS, Ballerup, Denmark), sanding, polishing with Forcipol 2V (Metkon, Bucharest, Romania), and attacking with chemical reagents. To work with this microscope, the prepared sample is placed on the table support plate, with the study surface facing up, ensuring the parallelism between the sample and the microscope table. The metallographic attack with chemical reagents highlights the crystalline structure by dissolving or selectively staining the various constituents present.

For polishing using the Forcipol 2V sanding/polishing machine, a time of 4 min was allocated on each metallographic paper (300, 500, 1000, 1500, 2000, 2500), with an application force: 20 N, using an emulsion with particles of diamond and a rotation speed of the platen of 200 rpm and the vector head of 60 rpm. The chemical etching fluid has the following composition: 10 mL HF, 5 mL HNO<sub>3</sub> and 85 mL H<sub>2</sub>O [24]. Due to the fact that the samples have undergone thermal treatment, the submersion time in the solution is approximately 5 s instead of 30 s (for non-treated titanium alloys).

### 2.4. Microhardness Test

The Vickers hardness tester is a Zwick 3212 microhardness (ZwickRoell GmbH, Ulm, Germany), presented in Figure 2. For the investigation of the alloys, the loading force will be from 0.2 to 1 kgf (small charge loads), which is why we are talking about the Vickers microhardness. The Vickers method consists in pressing on the surface of the test material a diamond penetrator, having the shape of a pyramid with a square base, with an angle between two opposite sides of 136°, with a reduced speed and a certain predetermined force. After indenting the sample, the device brings the objective of the measuring microscope over the remaining trace. The measurement of the trace diagonals (d1 and d2) is done with the help of the measuring eyepiece, the measuring accuracy being 0.5 µm. The diagonal of the trace is established as the arithmetic mean of the two measured diagonals. The Vickers hardness, symbolized by HV, is expressed by the ratio between the pressing force and the area of the lateral surface of the mark left by the penetrator on the part.

### 2.5. Indentation Test

Indentation is a common method for testing the mechanical characteristics of solid-state materials, such as their hardness and elastic stiffness, by observing how their surface interacts with the penetration of a probe with a defined geometry and applied stress.

To study the behavior of Ti-Mo-Zr-Ta alloys through the indentation test, the CETR UMT-2 tribometer (Center for Tribology, Campbell, CA, USA) was used. Samples with dimensions of 17 mm × 5 mm × 5 mm were used for the test. The samples were properly prepared by cutting, grinding, and polishing. The investigated samples were clamped on a flat surface of the testing apparatus with the help of screws and clamps. The tests were carried out in dry conditions. A Rockwell-type diamond indenter with a 120° indenter tip angle and 200 µm radius spherical tip was used, to which a force of 5 N was applied.



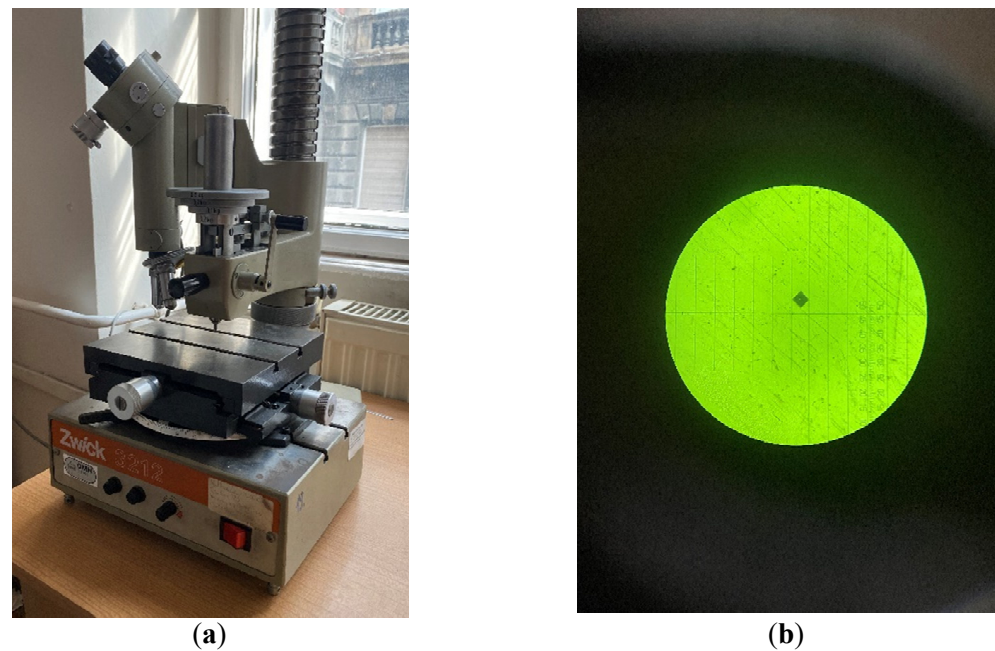


**Figure 2.** Hardness tester (a) front view (b) indented trace measurement.

### 3. Results and Discussions

#### 3.1. Heat Treatment Process

The heat treatment has been made following the diagram from Figure 3, which has been generated by the furnace operating system, based on the input values from Table 3.

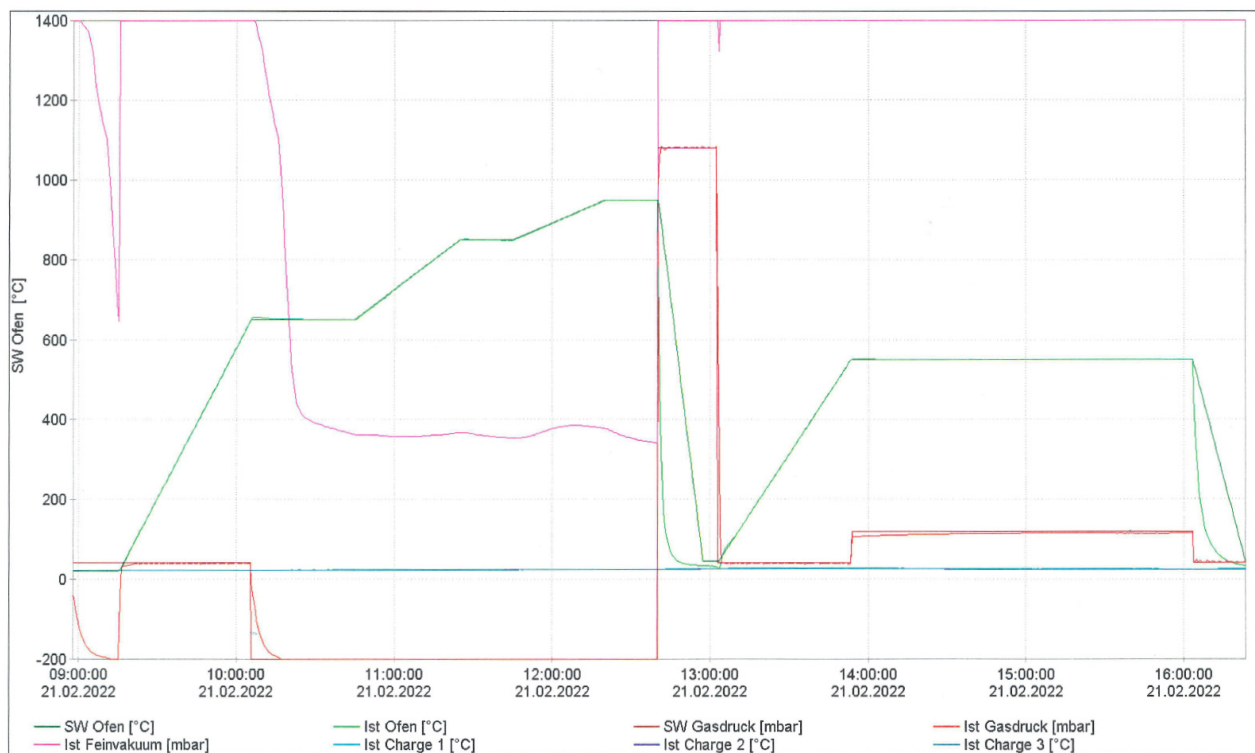


**Figure 3.** Heating diagram of the heat-treatment process (green—programmed and measured temperature, purple—vacuum, red—nitrogen pressure).

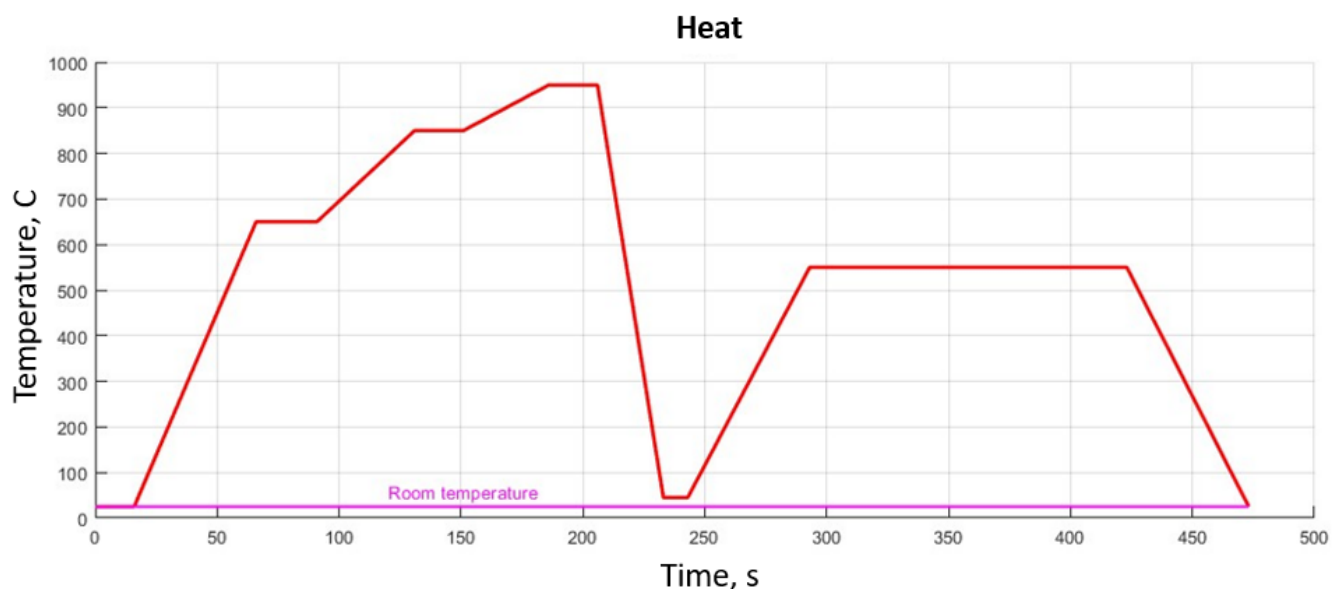
**Table 3.** Data input for the furnace charge diagram.

No.	Segment Name	Charge Diagram		Segment Name	Time
		Time	No.		
1	Vacuum	0:16	7	Dwell on heating at 950 °C	0:20
2	Heating on 650 °C	0:50	8	Cooling to 45 °C	0:17
3	Dwell on heating at 650 °C	0:25	9	Dwell on cooling at 45 °C	0:20
4	Heating on 850 °C	0:40	10	Heating on 550 °C	0:50
5	Dwell on heating at 850 °C	0:20	11	Dwell on heating at 550 °C	2:10
6	Heating on 950 °C	0:35	12	Cooling to room temperature	0:50

The heat treatment for the experiment has been conducted as follows:

- after locking the door to the furnace, a vacuum was achieved and maintained for 16 min in order to make sure that no residues or other chemicals were on the materials;
- a high-temperature quenching accomplished in three steps (650 °C—kept for 25 min, 850 °C—kept for 20 min, and 950 °C—kept for 20 min) and conducted in a vacuum in order to equalize the temperature between the middle and the core of the samples;
- the cooling process was achieved using N<sub>2</sub> gas, which was introduced in the chamber at a 9-bar pressure for 37 min;
- this was followed by heating to a constant temperature tempering (550 °C) at 1.5 bar pressure and kept for 2 h and 10 min at 2 bar pressure, as presented in Figure 4;
- after that, it was cooled at room temperature at a 1.5 bar pressure.

The purpose of such heat treatment can be, decreasing the level of internal tension induced in the metal mass of the products (stress relief annealing); recrystallization of the cross grain after cold plastic deformation or of the structure resulting from casting; finishing of overheated structures; reducing the hardness of the metallic material in order to improve workability.

**Figure 4.** Cont.

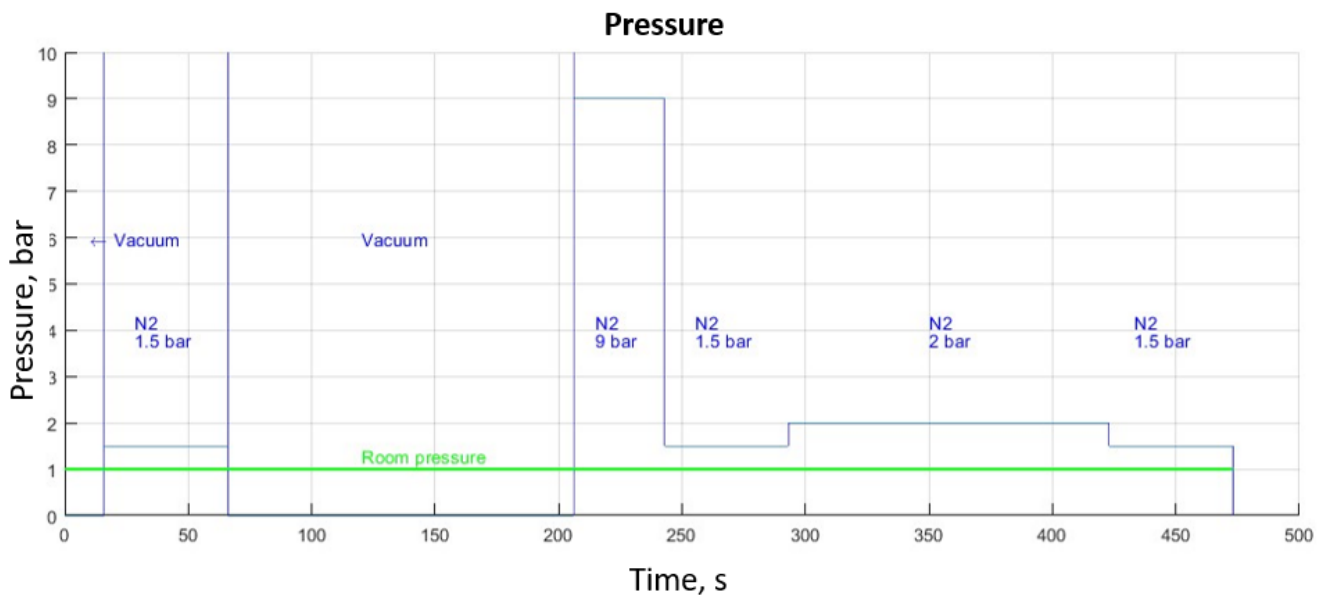


**Figure 4.** Extended heat and pressure diagrams generated in MATLAB.

### 3.2. Optical Microscopy Analysis

Figures 5 and 6 show the structure of Ti-Mo-Zr-Ta alloys with grain-specific aspects of titanium alloys. Optical microscopy images for Ti15Mo7Zr5Ta, Ti15Mo7Zr10Ta, and Ti15Mo7Zr15Ta highlight the lamellar dendrites inside the  $\beta$ -type grains. Ti20Mo7Zr5Ta, Ti20Mo7Zr10Ta, and Ti20Mo7Zr15Ta alloys show a dendritic structure with irregular grain boundaries. These acicular and coarse structures are specific to  $\beta$  alloys [24,25].

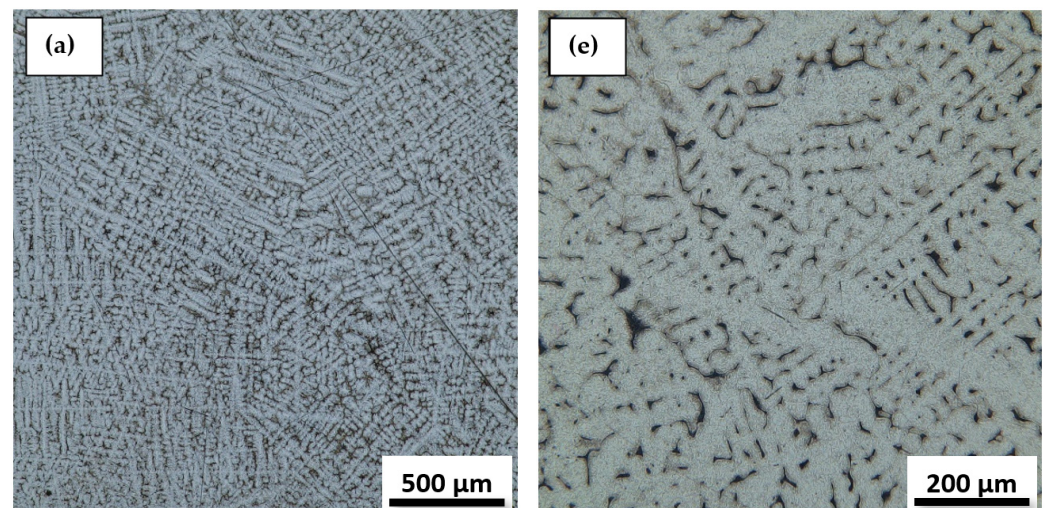


**Figure 5.** Cont.



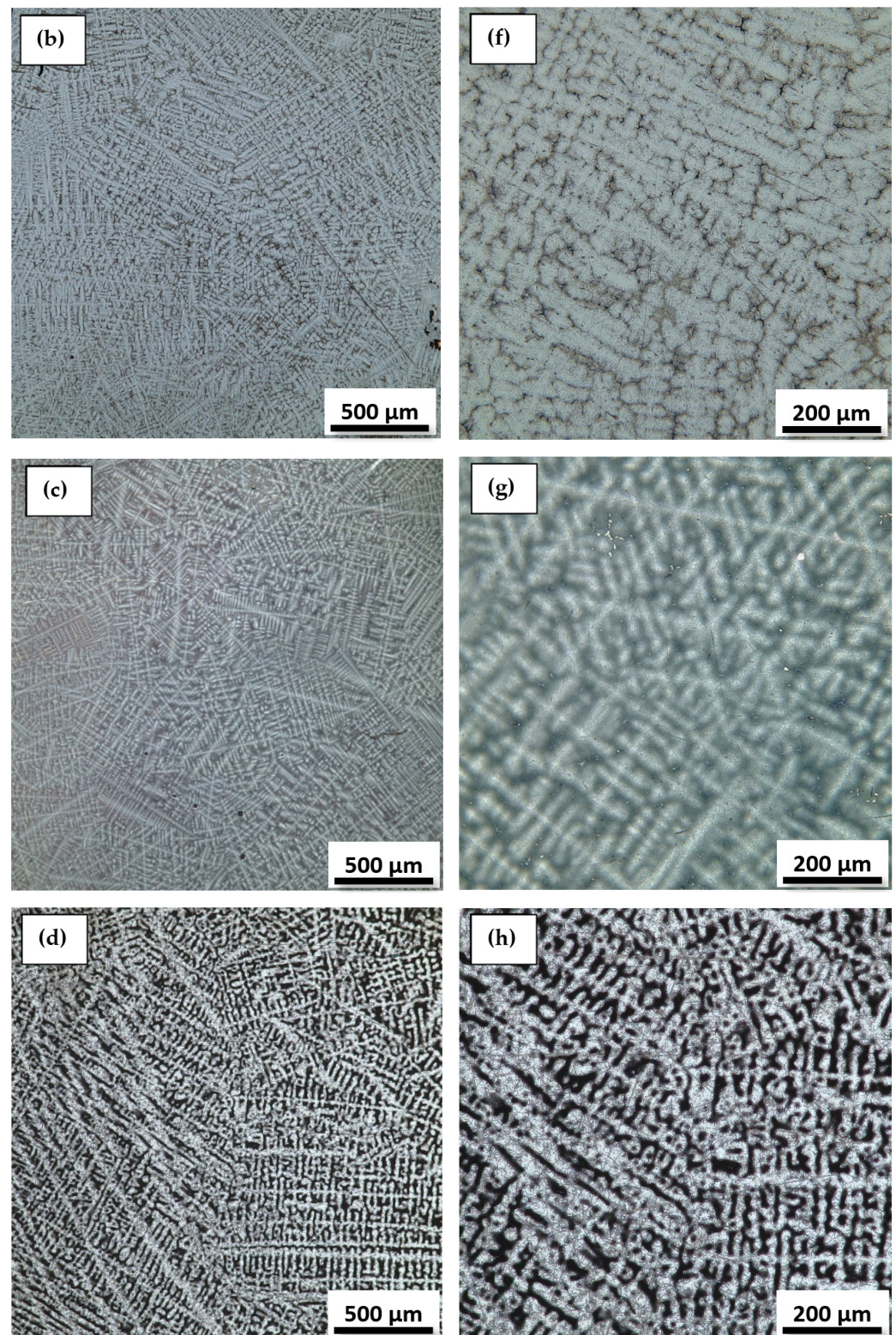


**Figure 5.** Microstructure analysis of Ti15Mo7Zr15Ta alloys with different percentage of Si added at a magnifying power of 70x: (a) Ti15Mo7Zr15Ta, (b) Ti15Mo7Zr15Ta0.5Si, (c) Ti15Mo7Zr15Ta0.75Si, (d) Ti15Mo7Zr15Ta1Si and of 280x: (e) Ti15Mo7Zr15Ta, (f) Ti15Mo7Zr15Ta0.5Si, (g) Ti15Mo7Zr15Ta0.75Si, (h) Ti15Mo7Zr15Ta1Si.



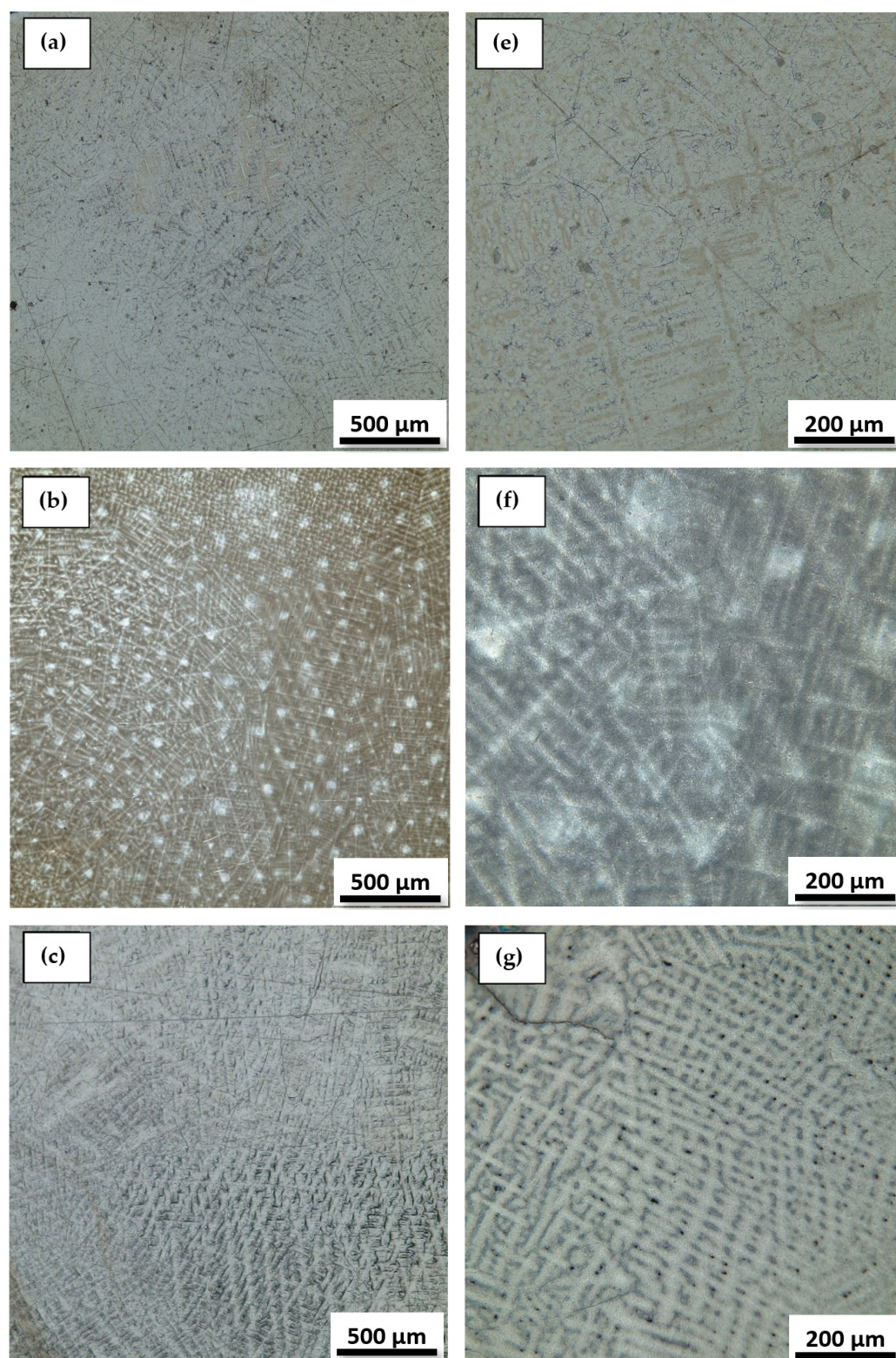
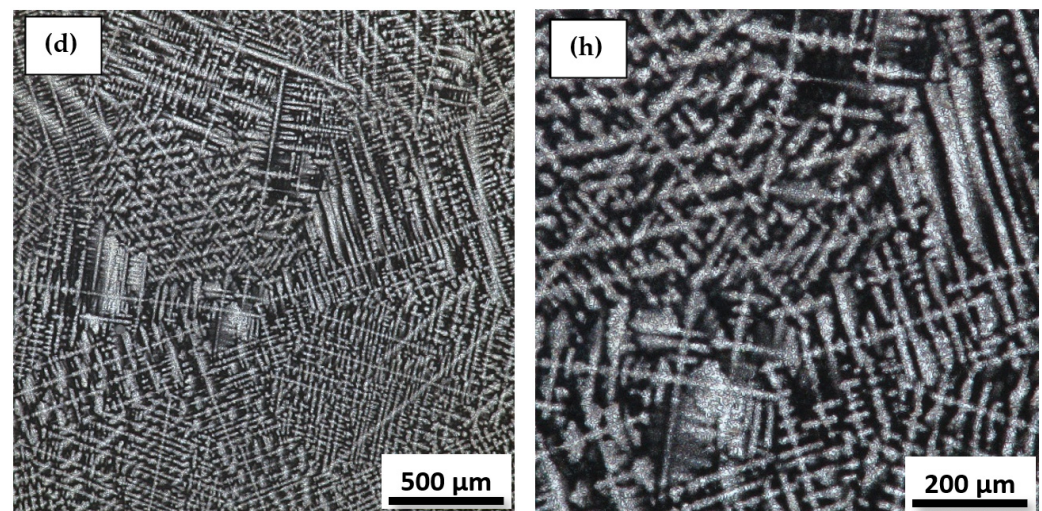


Figure 6. Cont.





**Figure 6.** Microstructure analysis of Ti20Mo7Zr15Ta alloys with different percentages of Si added at a magnifying power of 70x: (a) Ti20Mo7Zr15Ta, (b) Ti20Mo7Zr15Ta0.5Si, (c) Ti20Mo7Zr15Ta0.75Si, (d) Ti20Mo7Zr15Ta1Si and of 280x: (e) Ti20Mo7Zr15Ta, (f) Ti20Mo7Zr15Ta0.5Si, (g) Ti20Mo7Zr15Ta0.75Si, (h) Ti20Mo7Zr15Ta1Si.

At 882 °C, titanium undergoes an allotropic transformation, which allows the metal to transit from an  $\alpha$ -phase hexagonal close-packed structure to a  $\beta$ -phase body-centered cubic structure [26]. Due to molybdenum and tantalum stabilizers, studies have shown that  $\beta$ -phase alloys have the advantage of increased mechanical strength and an elastic modulus similar to human bone, both of which are important aspects of the long-term use of biomaterials in the medical field [27].

Thermal treatments are a sequence of stages that consist of the heating, maintenance, and cooling of some metal alloys to obtain certain structures that ensure the desired set of physico-chemical characteristics without changing the state of aggregation of the material [28–30].

Compared to other conventional biomaterials, Ti-Mo alloys containing various biocompatible components such as zirconium and tantalum have superior mechanical qualities such as high tensile strength and a significantly lower modulus of elasticity close to that of human bone. When the  $\alpha$  alloying elements are introduced into the titanium, the temperature at which the phase transition occurs changes [31,32]. The temperature range in which an  $\alpha$  phase rises when pure titanium is alloyed with  $\beta$  stabilizing elements (Mo, Ta, Si), whereas the alloy with elements expands the  $\beta$  phase domain. Other elements, such as zirconium, have a neutral effect on the temperature domains where the two phases coexist [33–35].

The images obtained by optical microscopy highlight a biphasic structure consisting of a high proportion of  $\beta$  solid solution, in which intergranular lamellar structures specific to  $\alpha''$  orthorhombic martensite appear (Figures 5 and 6).

The structure of the Ti-Mo-Zr-Ta alloys is similar to the microstructure of the commercial Ti-6Al-4V alloys. Typically, the Ti-6Al-4V microstructure contains  $\alpha$ -type very fine acicular needles,  $\alpha + \beta$  lamellar structures, and  $\beta$ -type grains [36,37]. In general, the microstructure of titanium alloys consists of a lamellar structure of  $\alpha$  and  $\beta$ . However, the  $\alpha$  morphology could change with heat treatment or depending on the amount of  $\beta$  elements added.

The lamellar microstructure, produced on cooling from the phase field, and the equiaxial microstructure, resulting from the recrystallization process, are the two extreme situations of phase arrangements, and they both affect the microstructure of titanium alloys. Much investigation has gone into how phase size and arrangement affect mechanical properties. With the increase of the volume fraction of the  $\beta$  phase, the strength of the alloy will increase, and the properties will be close to the human body [38].

The alloys presented a structure composed of dendrites that are typical of the phase structures  $\alpha''$  and grains characteristic of  $\beta$ -type alloys.  $\alpha''$  orthorhombic martensite frequently occurs in titanium-based alloys in which  $\beta$ -stabilizers from the transition metal category are found, including Mo, Nb, and Si. For our alloys, the presence of the  $\alpha''$  phase is due to the decomposition of the  $\beta$  phase during cooling.

### 3.3. Microhardness Results

For the Vickers microhardness method, at least ten tests are carried out on the material under test. For each trace, the average value of the diagonal is calculated based on the sizes of the two measured diagonals. The difference between the dimensions of the diagonals is allowed to be within a maximum margin of error of 2%. The samples were evaluated before and after the thermal treatment. The results are presented in Table 4 and Figure 7.

**Table 4.** Measured microhardness before and after the thermal treatment.

Alloy	Microhardness (HV)	
	Before Treatment	After Treatment
Ti15Mo7Zr15Ta	237.27 $\pm$ 5.3	375.75 $\pm$ 2.5
Ti15Mo7Zr15Ta0.5Si	343.98 $\pm$ 2.2	310.44 $\pm$ 3.6
Ti15Mo7Zr15Ta0.75Si	370.07 $\pm$ 1.5	373.63 $\pm$ 2.3
Ti15Mo7Zr15Ta1Si	364.24 $\pm$ 3.3	383.00 $\pm$ 3.1
Ti20Mo7Zr15Ta	305.34 $\pm$ 4.1	278.00 $\pm$ 5.2
Ti20Mo7Zr15Ta0.5Si	341.10 $\pm$ 2.8	360.38 $\pm$ 2.4
Ti20Mo7Zr15Ta0.75Si	318.20 $\pm$ 9.2	483.50 $\pm$ 6.7
Ti20Mo7Zr15Ta1Si	274.64 $\pm$ 1.8	391.13 $\pm$ 0.9

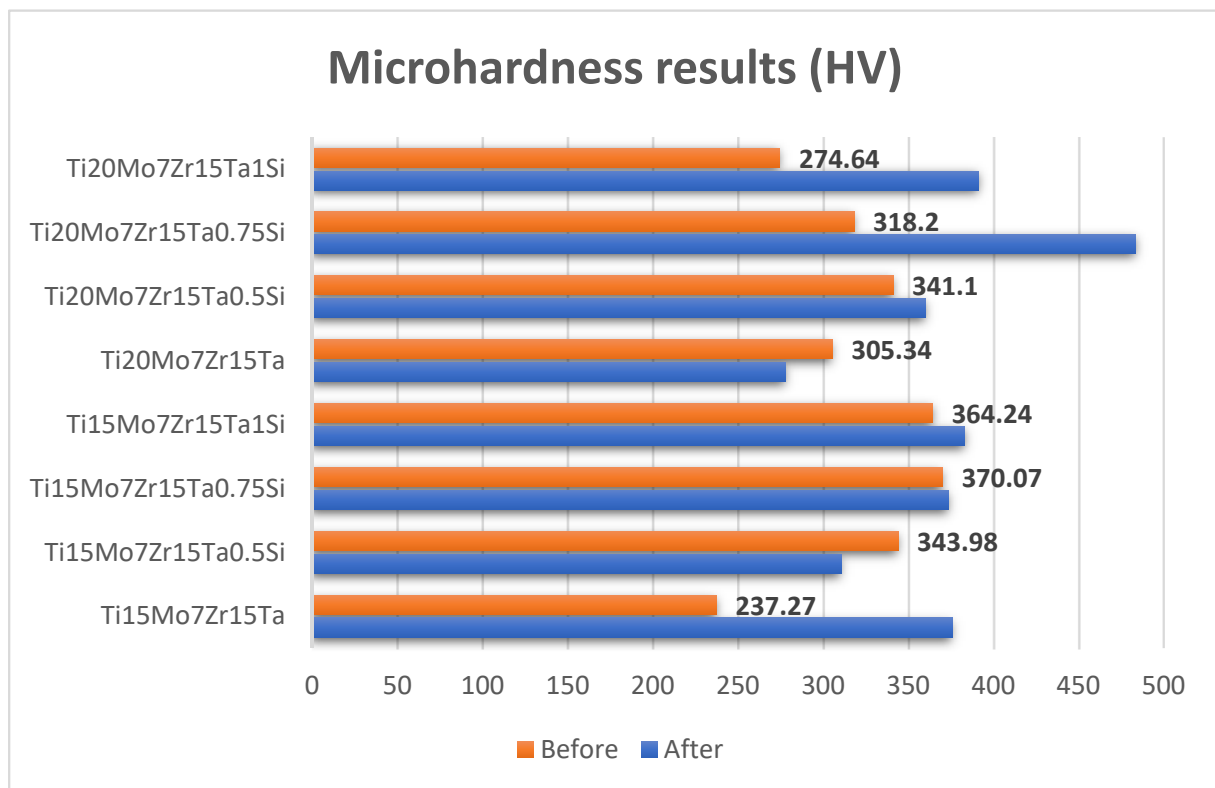


**Figure 7.** Hardness comparison (before and after the thermal treatment).

The results showed that the microhardness is significantly influenced by the heat treatment, with the exception of the Ti15Mo7Zr15Ta0.5Si and Ti20Mo7Zr15Ta alloys.

It can be observed that with the increase of the percentage of silicon and molybdenum by 20%, the hardness value after heat treatment is significantly increased, visible in the Ti20Mo7Zr15Ta0.75Si and Ti20Mo7Zr15Ta1Si alloys.

Microhardness studies on the surface show the depth of work hardening of the machined surface. The heating and cooling phenomena are the main cause of the microhardness growth on the surface and subsurface. The environment and cutting conditions impact the heating and cooling phenomenon. Due to grain refinement, the microhardness of machined surfaces rises. Since titanium alloys and nickel-based superalloys have a greater range of applications in the aerospace and biomedical areas, they have received a great deal of attention from researchers over the past ten years. Many of these articles have focused on the surface hardness of machined surfaces [11,16,17].

### 3.4. Indentation Results

The indentation test is a method to characterize the behavior of a material under a complex load. The applied load and displacement are measured during the test, while the residual footprint can be measured after the test has been completed. The results of this test are commonly used for material testing to determine the deformation resistance of a material.

Three determinations were made for each alloy for a more precise determination. The results of the modulus of elasticity of the Ti-Mo-Zr-Ta alloys are highlighted in Table 5.

**Table 5.** Indentation results.

Alloy	Loading Deformation [N]	Release Deformation [ $\mu\text{m}$ ]	Young Modulus [GPa]	Stiffness [N/ $\mu\text{m}$ ]	Specimen Poisson Ration
Ti15Mo7Zr15Ta	$13.52 \pm 0.2$	$10.39 \pm 0.1$	$41.89 \pm 0.3$	$2.03 \pm 0.1$	0.23
Ti15Mo7Zr15Ta0.5Si	$13.54 \pm 0.1$	$6.07 \pm 0.3$	$47.34 \pm 0.1$	$3.23 \pm 0.2$	0.23
Ti15Mo7Zr15Ta0.75Si	$13.54 \pm 0.2$	$6.73 \pm 0.4$	$66.24 \pm 0.1$	$4.26 \pm 0.1$	0.23
Ti15Mo7Zr15Ta1Si	$13.52 \pm 0.4$	$7.57 \pm 0.2$	$60.25 \pm 0.4$	$4.95 \pm 0.1$	0.23
Ti20Mo7Zr15Ta	$13.52 \pm 0.2$	$6.62 \pm 0.2$	$50.43 \pm 0.3$	$4.25 \pm 0.3$	0.23
Ti20Mo7Zr15Ta0.5Si	$13.53 \pm 0.3$	$6.79 \pm 0.3$	$54.65 \pm 0.2$	$4.56 \pm 0.1$	0.23
Ti20Mo7Zr15Ta0.75Si	$13.52 \pm 0.1$	$5.89 \pm 0.4$	$54.25 \pm 0.3$	$4.65 \pm 0.2$	0.23
Ti20Mo7Zr15Ta1Si	$13.54 \pm 0.2$	$6.72 \pm 0.4$	$36.25 \pm 0.4$	$4.35 \pm 0.1$	0.23

The modulus of elasticity obtained by the indentation method for the experimental alloys from the Ti-Mo-Zr-Ta system is between 36.25–66.24 GPa. The lowest value is presented by the Ti20Mo7Zr15Ta1Si alloy (38.57 GPa), and the highest value is presented by the Ti15Mo7Zr15Ta0.75Si alloy (66.24 GPa). The low values of the elastic modulus of the investigated alloys are due to the presence of  $\beta$ -stabilizing elements, such as Mo, Nb, and Si. According to the results in Table 5, as the Si content increases with a high content of 20% Mo, the modulus of elasticity decreases by about 30 GPa.

However, for medical applications aimed at replacing hard tissues, it is known that too much hardness leads to high wear, and too little modulus of elasticity prevents the uniform distribution of mechanical stresses, thus favoring bone resorption [2].

Great efforts are being made to produce implantable medical devices newly generated from Ti alloys that present a modulus of elasticity closer to that of bone and do not release ions with cytotoxic potential [3].

## 4. Conclusions

In this paper, the influence of heat treatment on the microstructure characteristics and mechanical properties of Ti-Mo-Zr-Ta alloys has been investigated. Thermal treatments are mainly used, focusing on superficial hardening, thus ensuring proper contact wear behavior; improving fatigue and corrosion resistance. The main results are as follows:



Regarding the microstructural analyses, the variation of the  $\alpha$ ,  $\alpha + \beta$ , and  $\beta$  type phases consists of differences in the chemical composition of the constituent elements.  $\beta$ -type structure formation is highlighted in Ti-Mo-Zr-Ta alloys, which contain a high percentage of  $\beta$  stabilizing elements (Mo, Ta, Si). Zirconium in concentrations below 7% also contributes to the refinement of the microstructure, thus allowing the formation of a homogeneous and evenly distributed structure. Therefore, elements like tantalum (5–15%), molybdenum (15–20%) and silicon in different concentrations (0.5, 0.75, and 1%), contribute to the formation of the  $\beta$  phase at titanium alloys.

Based on the microhardness testing, it was observed that the hardness of some alloys has increased by approximately 5% for Ti15Mo7Zr15Ta1Si and Ti20Mo7Zr15Ta0.5Si, while for Ti15Mo7Zr15Ta0.5Si and Ti20Mo7Zr15Ta an approximately 9% decrease has been noted. At the same time, a slight increase of 0.9% has been observed for Ti15Mo7Zr15Ta0.75Si. An influence of the heat treatment is highlighted in Ti15Mo7Zr15Ta, Ti20Mo7Zr15Ta0.75Si, and Ti20Mo7Zr15Ta1Si; these changes come from the concentration of each beta stabilizer on the alloys.

The results of the indentation test on the Ti-Mo-Zr-Ta alloys highlighted a reduced modulus of elasticity compared to the classic alloys, identifying the Ti20Mo7Zr15Ta1Si alloy (38.57 GPa) with the lowest value close to the human bone (15–30 GPa).

In conclusion, the application of thermal treatments aims to achieve the proper properties of the metallic product in efficient economic and technical conditions. An improvement in hardness was seen in the alloys and a low modulus of elasticity, recommending them as alloys for orthopedic implants.

**Author Contributions:** M.S.B.: conceptualization, management; C.C.-M.: writing—original draft preparation, investigation; P.V.: methodology, financing, data curation; L.T.: investigation, writing—review and editing; J.N.: validation, investigation. All authors have read and agreed to the published version of the manuscript.

**Funding:** This work was supported by a innovations grant of the TUIASI, project number MedTech\_8/2022.

**Institutional Review Board Statement:** Not applicable.

**Informed Consent Statement:** Not applicable.

**Data Availability Statement:** All data provided in the present manuscript are available to whom it may concern.

**Conflicts of Interest:** The authors declare no conflict of interest.

## References

1. Encyclopaedia Britannica. Available online: <https://www.britannica.com/science/titanium> (accessed on 13 April 2022).
2. Chen, Q.; Thouas, G.A. Metallic implant biomaterials. *Mater. Sci. Eng. R* **2015**, *87*, 1–57. [CrossRef]
3. Vizureanu, P.; Bălțatu, M.S. *Titanium-Based Alloys for Biomedical Applications*; Materials Research Forum LLC: Millersville, PA, USA, 2020; Volume 74.
4. González, J.E.G.; Mirza-Rosca, J.C. Study of the corrosion behavior of titanium and some of its alloys for biomedical and dental implant applications. *J. Electroanal. Chem.* **1999**, *471*, 109–115. [CrossRef]
5. Kaur, M.; Singh, K. Review on titanium and titanium based alloys as biomaterials for orthopaedic applications. *Mater. Sci. Eng. C* **2019**, *102*, 844–862. [CrossRef] [PubMed]
6. Quinn, J.; McFadden, R.; Chan, C.W.; Carson, L. Titanium for orthopedic applications: An overview of surface modification to improve biocompatibility and prevent bacterial biofilm formation. *iScience* **2020**, *23*, 101745. [CrossRef] [PubMed]
7. Munteanu, C.; Vlad, D.M.; Sindilar, E.-V.; Istrate, B.; Butnaru, M.; Pasca, S.A.; Nastasa, R.O.; Mihai, I.; Burlea, S.-L. Novel Mg-0.5Ca-xMn biodegradable alloys intended for orthopedic application: An in vitro and in vivo study. *Materials* **2021**, *14*, 7262. [CrossRef]
8. Civantos, A.; Martínez-Campos, E.; Ramos, V.; Elvira, C.; Gallardo, A.; Abarrategi, A. Titanium coatings and surface modifications: Toward clinically useful bioactive implants. *ACS Biomater. Sci. Eng.* **2017**, *3*, 1245–1261. [CrossRef]
9. Korkmaz, M.E.; Gupta, M.K.; Waqar, S.; Kuntoglu, M.; Krolczyk, G.M.; Maruda, R.W.; Pimenov, D.Y. A short review on thermal treatments of Titanium & Nickel based alloys processed by selective laser melting. *J. Mater. Res. Technol.* **2022**, *16*, 1090–1101. [CrossRef]

10. Wang, C.; Li, B.; Wang, T.; Qi, P.; Qiao, X.; Yin, J.; Nie, Z. Microtexture evolution effected by Mo content in  $\alpha + \beta$  titanium alloys. *Mater. Charact.* **2022**, *188*, 111884. [\[CrossRef\]](#)
11. Wang, W.; Liang, S.Y. A 3D analytical modeling method for keyhole porosity prediction in laser powder bed fusion. *Int. J. Adv. Manuf. Technol.* **2022**, *120*, 3017–3025. [\[CrossRef\]](#)
12. Popa, M.V.; Vasilescu, E.; Drob, P.; Vasilescu, C.; Drob, S.I.; Mareci, D.; Mirza Rosca, J.C. Corrosion resistance improvement of titanium base alloys. *Quim. Nova* **2010**, *33*, 1892–1896. [\[CrossRef\]](#)
13. Verma, R.P. Titanium based biomaterial for bone implants: A mini review. *Mater. Today Proc.* **2020**, *26*, 3148–3151. [\[CrossRef\]](#)
14. Bitay, E.; Tóth, L.; Kovács, T.A.; Nyikes, Z.; Gergely, A.L. Experimental study on the influence of TiN/AlTiN PVD layer on the surface characteristics of hot work tool steel. *Appl. Sci.* **2021**, *11*, 9309. [\[CrossRef\]](#)
15. Stefanescu, D.; Ruxandra, R. Metallography and microstructures, book chapter: Solidification structures of titanium alloys. *ASM Int.* **2004**, *9*, 116–126. [\[CrossRef\]](#)
16. Baltatu, M.S.; Vizureanu, P.; Balan, T.; Lohan, N.M.; Tugui, C.A. Preliminary tests for Ti-Mo-Zr-Ta alloys as potential biomaterials. *IOP Conf. Ser. Mater. Sci. Eng.* **2018**, *374*, 012023. [\[CrossRef\]](#)
17. Băltatu, I.; Vizureanu, P.; Ciolacu, F.; Achîţei, D.C.; Băltatu, M.S.; Vlad, D. In vitro study for new Ti-Mo-Zr-Ta alloys for medical use. *IOP Conf. Ser. Mater. Sci. Eng.* **2019**, *572*, 012030. [\[CrossRef\]](#)
18. Bagmutov, V.P.; Vodopyanov, V.I.; Zakharov, I.N.; Ivannikov, A.Y.; Bogdanov, A.I.; Romanenko, M.D.; Barinov, V.V. Features of changes in the surface structure and phase composition of the of alpha plus beta titanium alloy after electromechanical and thermal treatment. *Metals* **2022**, *12*, 1535. [\[CrossRef\]](#)
19. Wang, C.; Li, B.; Wang, T.; Qi, P.; Qiao, X.; Yin, J.; Nie, Z. Microstructure and thermal stability of high-temperature titanium alloy with Hf element. *Adv. Eng. Mater.* **2022**, 2200337. [\[CrossRef\]](#)
20. Weng, W.; Biesiekierski, A.; Li, Y.; Wen, C. Effects of selected metallic and interstitial elements on the microstructure and mechanical properties of beta titanium alloys for orthopedic applications. *Materialia* **2019**, *6*, 100323. [\[CrossRef\]](#)
21. Spataru, M.C.; Cojocaru, F.D.; Sandu, A.V.; Solcan, C.; Duceac, I.A.; Baltatu, M.S.; Voiculescu, I.; Geanta, V.; Vizureanu, P. Assessment of the effects of Si addition to a new TiMoZrTa system. *Materials* **2021**, *14*, 7610. [\[CrossRef\]](#)
22. Verestiuc, L.; Spataru, M.C.; Baltatu, M.S.; Butnaru, M.; Solcan, C.; Sandu, A.V.; Voiculescu, I.; Geanta, V.; Vizureanu, P. New Ti-Mo-Si materials for bone prosthesis applications. *J. Mech. Behav. Biomed. Mater.* **2021**, *113*, 104198. [\[CrossRef\]](#)
23. Schmetz. Available online: <https://www.schmetz.de/en/products/horizontal-high-temperature-vacuum-chamber-furnace.html> (accessed on 25 March 2022).
24. Sandu, A.V.; Băltatu, M.S.; Nabialek, M.; Savin, A.; Vizureanu, P. Characterization and mechanical proprieties of new TiMo alloys used for medical applications. *Materials* **2019**, *12*, 2973. [\[CrossRef\]](#) [\[PubMed\]](#)
25. Zhou, Y.L.; Luo, D.M. Microstructures and mechanical properties of Ti-Mo alloys cold-rolled and heat treated. *Mater. Charact.* **2011**, *62*, 931–937. [\[CrossRef\]](#)
26. Yadav, P.; Saxena, K.K. Effect of heat-treatment on microstructure and mechanical properties of Ti alloys: An overview. *Mater. Today Proc.* **2020**, *26*, 2546–2557. [\[CrossRef\]](#)
27. Geetha, M.; Singh, A.K.; Asokamani, R.; Gogia, A.K. Ti based biomaterials, the ultimate choice for orthopaedic implants—A review. *Mater. Sci.* **2009**, *54*, 397–425. [\[CrossRef\]](#)
28. Zhang, L.C.; Chen, L.Y. A review on biomedical titanium alloys: Recent progress and prospect. *Adv. Eng. Mater.* **2019**, *21*, 1801215. [\[CrossRef\]](#)
29. Jiang, Z.; Dai, X.; Middleton, H. Effect of silicon on corrosion resistance of Ti-Si alloys. *Mater. Sci. Eng. B* **2011**, *176*, 79–86. [\[CrossRef\]](#)
30. Baltatu, M.S.; Vizureanu, P.; Sandu, A.V.; Munteanu, C.; Istrate, B. Microstructural analysis and tribological behavior of Ti-based alloys with a ceramic layer using the thermal spray method. *Coatings* **2020**, *10*, 1216. [\[CrossRef\]](#)
31. Sharman, K.; Bazarnik, P.; Brynk, T.; Bulutsuz, A.G.; Lewandowska, M.; Huang, Y.; Langdon, T.G. Enhancement in mechanical properties of a  $\beta$ -titanium alloy by high-pressure torsion. *J. Mater. Res. Technol.* **2015**, *4*, 79–83. [\[CrossRef\]](#)
32. Kartika, I.; Rokhmanto, F.; Thaha, Y.N.; Purawardi, I.; Astawa, I.N.G.P.; Erryani, A.; Asmaria, T. Influence of thermo-mechanical processing on microstructure, mechanical properties and corrosion behavior of Ti-6Al-6Mo implant alloy. In Proceedings of the 1st International Conference on Electronics, Biomedical Engineering, and Health Informatics, Surabaya, Indonesia, 8–9 October 2020; Springer: Berlin/Heidelberg, Germany, 2021; pp. 397–405. [\[CrossRef\]](#)
33. Eisenbarth, E.; Velten, D.; Müller, M.; Thull, R.; Breme, J. Biocompatibility of  $\beta$ -stabilizing elements of titanium alloys. *Biomaterials* **2004**, *25*, 5705–5713. [\[CrossRef\]](#)
34. Wang, J.; Liu, Y.; Rabadia, C.D.; Liang, S.X.; Sercombe, T.B.; Zhang, L.C. Microstructural homogeneity and mechanical behavior of a selective laser melted Ti-35Nb alloy produced from an elemental powder mixture. *J. Mater. Sci. Technol.* **2021**, *61*, 221–233. [\[CrossRef\]](#)
35. Padhy, G.K.; Wu, C.S.; Gao, S. Friction stir based welding and processing technologies—Processes, parameters, microstructures and applications: A review. *J. Mater. Sci. Technol.* **2018**, *34*, 1–38. [\[CrossRef\]](#)
36. Razavykia, A.; Brusa, E.; Delprete, C.; Yavari, R. An overview of additive manufacturing technologies—A review to technical synthesis in numerical study of selective laser melting. *Materials* **2020**, *13*, 3895. [\[CrossRef\]](#) [\[PubMed\]](#)

- 
37. Zhong, C.; Liu, J.; Zhao, T.; Schopphoven, T.; Fu, J.; Gasser, A.; Schleifenbaum, J.H. Laser metal deposition of Ti6Al4V—A brief review. *Appl. Sci.* **2020**, *10*, 764. [[CrossRef](#)]
  38. Kumar, V.A.; Gupta, R.; Prasad, M.; Murty, S.N. Recent advances in processing of titanium alloys and titanium aluminides for space applications: A review. *J. Mater. Res.* **2021**, *36*, 689–716. [[CrossRef](#)]